

Measurement of the differential distributions of $B_s^0 \rightarrow D_s^{*-} \mu^+ \nu_\mu$ decay with the LHCb detector

Patrizia de Simone,^a Federico Manganello^{a,b,*} and Marcello Rotondo^a for the LHCb collaboration

^aLaboratori Nazionali di Frascati

^bINFN & Università Tor Vergata

E-mail: patrizia.de.simone@lnfn.infn.it,

federico.manganello@roma2.infn.it, marcello.rotondo@lnfn.infn.it

This analysis aims to conduct a comprehensive study of the decay kinematics of the semileptonic decay $B_s^0 \rightarrow D_s^{*-} \mu^+ \nu_\mu$, with $D_s^{*-} \rightarrow D_s^- \gamma$ and $D_s^- \rightarrow K^+ K^- \pi^-$, using data collected by the LHCb experiment in Run 2. A first measurement of the form factors describing the B_s^0 meson semileptonic decay is provided, performing a four-dimensional binned fit in the space given by the variables describing the decay kinematics, namely q^2 , $\cos \theta_\ell$, $\cos \theta_d$ and χ . Taking into account the detector acceptance, as well as the reconstruction efficiencies and the resolution effects, the full differential distribution is obtained; then, a fit to this distribution is performed using different parameterizations for the $B_s^0 \rightarrow D_s^*$ transition form factors. Furthermore, the unfolded distributions are compared with the theoretical predictions and the Belle-II experiment results. Finally, using the unfolded shapes, a model-independent approach is tested and its compatibility with the model-dependent results is studied.

Third Italian Workshop on the Physics at High Intensity
12-15 November 2024
Bologna, Italy

*Speaker

© Copyright owned by the author(s) under the terms of the Creative Commons Attribution-NonCommercial-NoDerivatives 4.0 International License (CC BY-NC-ND 4.0). All rights for text and data mining, AI training, and similar technologies for commercial purposes, are reserved. ISSN 1824-8039. Published by SISSA Medialab.

<https://pos.sissa.it/>

1. Introduction

The b -hadrons semileptonic decays are a powerful tool for investigating and probing the Standard Model (SM). They are referred to as $H_b \rightarrow H_c \ell \nu$, where the hadron H_b containing a b quark decays into a charmed hadron H_c , a charged lepton ℓ and a neutrino ν . In the SM, these decays proceed via tree-level charged currents, mediated by a W boson. Due to the strong interaction between the decaying and the spectator quarks, these processes provide access to both the Electroweak and Strong sectors of the SM. Furthermore, potential New Physics (NP) interactions, such as lepto-quarks [1] or charged Higgs bosons [2], may interfere with or mediate these processes. For this reason, precise measurements of these decay properties are essential.

This study investigates the semileptonic decay $B_s^0 \rightarrow D_s^{*-} \mu^+ \nu_\mu$ and the charge-conjugate decay, with $D_s^{*-} \rightarrow D_s^- \gamma$ and $D_s^- \rightarrow K^+ K^- \pi^-$, with data collected by the LHCb experiment during the Run 2 data-taking period (2016-2018). The analysis aims to measure the differential decay rate described by four kinematic variables: the squared momentum q^2 transferred to the lepton pair, two helicity angles θ_ℓ and θ_d associated with the decays of the W and D_s^* in their reference frames, and a third angle χ between these two decay planes. A previous one-dimensional analysis was already performed in LHCb using a subset of the Run 2 dataset [3].

As detailed in several studies (e.g. [4]), the complete differential decay rate is given by

$$\frac{d\Gamma}{dq^2 d\cos\theta_\ell d\cos\theta_d d\chi} = \mathcal{N}_\gamma |\vec{p}_{D_s^*}(q^2)| \left(1 - \frac{m_\mu^2}{q^2}\right)^2 \sum_i I_i(q^2) \Xi_i(\theta_\ell, \theta_d, \chi) \quad (1)$$

where \mathcal{N}_γ is a constant factor depending on $|V_{cb}|^2$ and the index i runs over several contributions. While the functions Ξ_i are well-known angular terms, the functions $I_i(q^2)$ describe the hadronic interaction between the spectator and the decaying quarks and are related to the helicity amplitudes H_t , H_\pm and H_0 : since the strong interaction is highly non-perturbative at low energies, a specific model is needed to parametrise their expression. In this analysis, we consider the Caprini-Lellouch-Neubert (CLN) [5] and the Boyd-Grinstein-Lebed (BGL) [6] models, as they are the most widely employed parameterizations. We also intend to implement a model-independent approach to direct comparisons with present and future LQCD calculations.

2. Event selection

Data collected by the LHCb experiment are a mixture of signal and background events, with the latter given by different processes that share the same final state as the signal: a charged muon, a reconstructed c -hadron with opposite charge, and a non-vanishing missing energy due to the neutrino and non-reconstructed particles. The trigger selection filters events containing a high momentum muon candidate, namely $p > 3$ GeV/ c . Moreover, high purity in the selected dataset can be achieved by applying additional selection cuts. First, in the Dalitz plot, only the ϕ and K^* resonances are selected, to identify the D_s^- properly. Then, the D_s^{*-} is reconstructed by considering photons inside a narrow cone surrounding the D_s^- candidate, defined in terms of pseudorapidity and azimuthal angle: only the photon with the highest momentum inside the cone is selected.

A fit to the $D_s^- \gamma$ invariant mass distribution, with the reconstructed D_s^- mass constrained to its known value [7], is then performed as shown in Fig. 1 (left). The signal is described by a one-sided

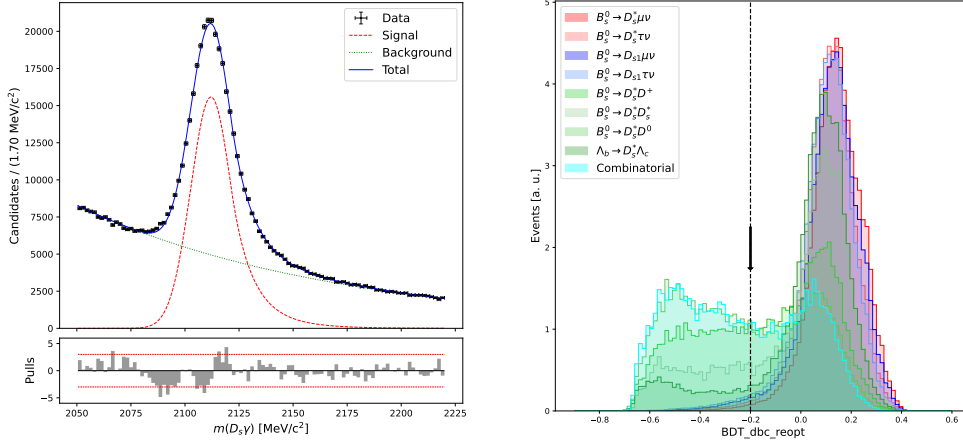


Figure 1: Left: sPlot on the D_s^* invariant mass on the data sample; right: distributions of the BDT variable for all the MC samples.

Crystal Ball function, over an exponential combinatorial background. The $s\mathcal{P}$ lot technique [8] is employed to subtract the combinatorial background from random photons. To further refine the selection, a cut over a Boosted-Decision Tree (BDT) variable is applied. The BDT is built using topological information about the process and is highly effective in rejecting the so-called doubly-charmed processes, where a b -hadron decays in a c -hadron and a D_s^* , with the latter decaying semileptonically. The shape of the BDT variable for the signal and background channels is shown in Fig. 1 (right). A cut at $\text{BDT_dbc_reopt} > -0.2$ is chosen to maximise the significance, resulting in a mean rejection efficiency of 60% on the doubly-charmed decays (the green shapes in figure).

3. Kinematic reconstruction

The presence of a neutrino in the final state poses a significant challenge in the LHCb environment. Since the detector does not provide full 4π -coverage, it is generally impossible to directly measure the missing momentum, which means that the kinematic system cannot be fully constrained. However, by assuming the known mass of the B_s^0 meson and the presence of only one massless particle in the final state, as demonstrated in [9] and [10], it becomes possible to determine the kinematic variables up to a quadratic ambiguity. In principle, one could randomly select one of the two solutions, but a 10% improvement in q^2 resolution can be achieved by employing a Multi-Variate Analysis (MVA) method. In this study, four different architectures were tested, with the best performance achieved by a Multi-Layer Perceptron (MLP). The regression algorithm provides a rough estimate of the B_s^0 momentum: to resolve the two-fold ambiguity, we select the solution closest to this estimate across all kinematic variables.

4. Signal yields

The central core of the analysis, which leads to our first results, is based on a four-dimensional binned fit in the corrected mass M_{corr} space. This variable is defined as

$$M_{corr} = \sqrt{m_{vis}^2 + |p_{vis}^\perp|^2 + |p_{vis}^\parallel|^2} \quad (2)$$

where m_{vis} is the visible invariant mass, namely $m_{D_s \gamma}$, and p_{vis}^\perp is the transverse visible momentum, i.e. the component of the visible momentum perpendicular to the B_s^0 flight direction. The M_{corr} plays a crucial role in angular analyses [11], since it provides an excellent tool to distinguish between signal and background processes. This is clearly illustrated in Fig. 2, where the signal distribution (in red) shows a distinct shape compared to background channels. The analysis strategy involves binning the parameter space and, within each bin, extracting the number of events for each channel by rescaling the simulated probability density functions (or templates) using a scale factor a_i^δ . These scale factors are free parameters of the fit, the subscript i refers to the channel and the index δ identifies a specific bin in the four-dimensional space. To improve the stability of the fit, the doubly-charmed templates are combined, as well as the $B_s^0 \rightarrow D_{s1} \ell \nu_\ell$ channels. Additionally, the combinatorial background — resulting from random combinations of hadrons and muons from different decays — is modeled using the events where the reconstructed D_s and μ are selected with the same electric charge. We decide to proceed in two steps:

- a simultaneous fit across the six different q^2 bins, integrating over the angular variables, and ending up with fifteen free parameters;
- independent fits across the 270 bins in the four-dimensional space, where the background components are fixed to the results of the first step, leaving only the signal scale factors as free parameters.

This two-step approach ensures a stable and reliable extraction of signal yields, mitigating the low-statistics challenges often encountered in multidimensional binned fits. An example of the result in the first set of fits is shown in Fig. 2 (the two plots on the left), while the results in two different bins of the multidimensional parameter space are shown in the same figure in the two plots on the right. It is noteworthy that the statistics significantly varies between different bins of the multidimensional parameter space, nevertheless all the fits show good agreement with the data, as pointed out by the pulls.

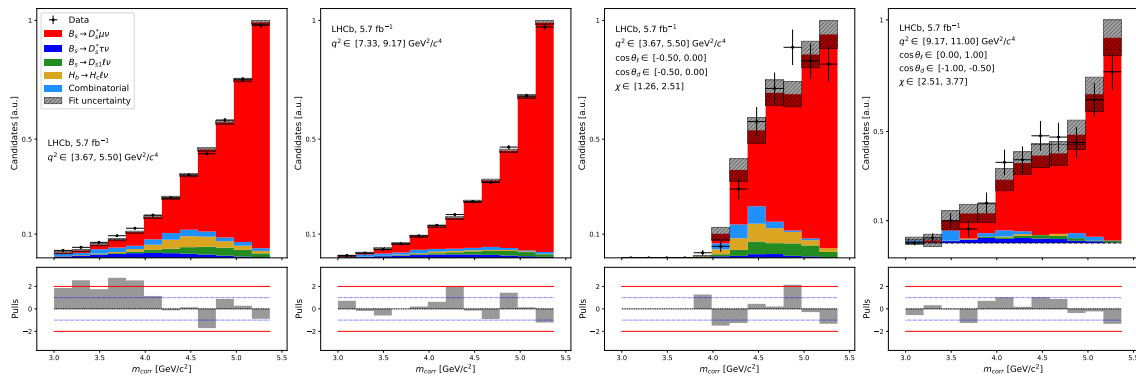


Figure 2: First two figures on the left: examples of fit in two different q^2 bins; on the right: examples of fit in two different bins in the 4-d space.

5. Conclusions

This angular analysis extends and improves a previously published analysis of the measurement of the q^2 spectrum for the $B_s^0 \rightarrow D_s^{*-} \mu^+ \nu_\mu$ semileptonic decays, with the data collected by the LHCb experiment. The differential decay rate extracted here is essential to conduct several studies. Notably, taking into account the detector's efficiency and resolution, as described in [12], it is possible to unfold and compare it with the theoretical models. In particular, Fig. 3 shows the comparison between experimental unfolded shapes and the CLN and BGL predicted shapes. A deviation in the q^2 distribution was already observed by Belle-II [13], even though in that case the $B \rightarrow D$ transition was under study. It is worth mentioning that we expect the experimental shapes to disagree with the predictions, since the theoretical computations are made taking into account the B^0 and not the B_s^0 meson.

Assuming the two different theoretical models we can extract the $I_i(q^2)$ functions. Additionally, the integrals of these functions in the q^2 bins can be extracted with a model-independent approach. This is possible since we know that the predicted signal yield, integrating Eq. 1 in a specific bin of the four-dimensional space, is given by

$$\begin{aligned} N_{k,p,q,r}^{\text{pred}} &= \int_{\Delta q_k^2} \int_{\Delta \cos \theta_{\ell p}} \int_{\Delta \cos \theta_{dq}} \int_{\Delta \chi_r} \frac{d\Gamma}{dq^2 d\cos \theta_{\ell} d\cos \theta_d d\chi} dq^2 d\cos \theta_{\ell} d\cos \theta_d d\chi \\ &\propto \sum_i \int_{\Delta q_k^2} \left(1 - m_\mu^2/q^2\right)^2 |\vec{p}_{D_s^*}(q^2)| I_i(q^2) dq^2 \cdot \int_{\Delta \Omega_i} \Xi_i(\theta_{\ell}, \theta_d, \chi) d\Omega \\ &\propto \sum_i J_{i,k}(q^2) \cdot \zeta_{i,l}(\theta_{\ell}, \theta_d, \chi) \end{aligned}$$

The angular integrals are well-known and analytically computable, and we can treat the $J_{i,k}(q^2)$ integrals as free parameters and compare them with the predictions of a specific model. This approach is highly valuable since we expect some of these functions to be zero in the SM framework, enabling direct measurement of deviations from SM and testing NP scenarios. We found the model-dependent and the model-independent approaches yield to compatible results, i. e. with relative deviations in the CLN parameters remaining below 1%.

Finally, we intend to conduct several other studies to understand the impact of NP models, for instance using the forward-backward asymmetry $\mathcal{A}_{FB}(q^2)$ [4] or the dimensionless quantities described in [14], which are model-independent and don't require the determination of the $|V_{cb}|$ constant.

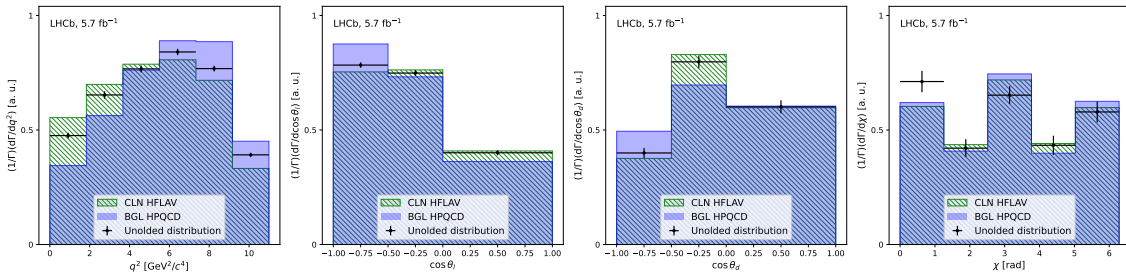


Figure 3: Experimental unfolded distributions and comparison with CLN and BGL models.

References

- [1] A. Angelescu, D. Bečirević, D. A. Faroughy, and O. Sumensari, “Closing the window on single leptoquark solutions to the b-physics anomalies”, *Journal of High Energy Physics*, vol. 2018, no. 10, p. 183, 2018. doi: [10.1007/JHEP10\(2018\)183](https://doi.org/10.1007/JHEP10(2018)183).
- [2] M. Tanaka, “Charged higgs effects on exclusive semi-tauonicb decays”, *Zeitschrift für Physik C Particles and Fields*, vol. 67, no. 2, pp. 321–326, Jun. 1995, ISSN: 1434-6052. doi: [10.1007/bf01571294](https://doi.org/10.1007/bf01571294).
- [3] R. Aaij *et al.*, “Measurement of the shape of the $B_s^0 \rightarrow D_s^{*-} \mu^+ \nu_\mu$ differential decay rate”, *Journal of High Energy Physics*, vol. 2020, no. 12, Dec. 2020. doi: [10.1007/jhep12\(2020\)144](https://doi.org/10.1007/jhep12(2020)144).
- [4] P. Colangelo and F. De Fazio, “Scrutinizing $\bar{B} \rightarrow D^* (D\pi) \ell^- \bar{\nu}_\ell$ and $\bar{B} \rightarrow D^* (D\gamma) \ell^- \bar{\nu}_\ell$ in search of new physics footprints”, *JHEP*, vol. 06, p. 082, 2018. doi: [10.1007/JHEP06\(2018\)082](https://doi.org/10.1007/JHEP06(2018)082).
- [5] I. Caprini, L. Lellouch, and M. Neubert, “Dispersive bounds on the shape of form factors”, *Nuclear Physics B*, vol. 530, no. 1-2, pp. 153–181, Oct. 1998. doi: [10.1016/s0550-3213\(98\)00350-2](https://doi.org/10.1016/s0550-3213(98)00350-2).
- [6] C. G. Boyd, B. Grinstein, and R. F. Lebed, “Model independent determinations of anti-B \rightarrow D (lepton), D^* (lepton) anti-neutrino form-factors”, *Nucl. Phys. B*, vol. 461, pp. 493–511, 1996. doi: [10.1016/0550-3213\(95\)00653-2](https://doi.org/10.1016/0550-3213(95)00653-2).
- [7] S. Navas *et al.*, “Review of particle physics”, *Phys. Rev. D*, vol. 110, no. 3, p. 030001, 2024. doi: [10.1103/PhysRevD.110.030001](https://doi.org/10.1103/PhysRevD.110.030001).
- [8] M. Pivk and F. L. Diberder, “ \mathcal{P} Plot: A statistical tool to unfold data distributions”, *Nuclear Instruments and Methods in Physics Research Section A: Accelerators, Spectrometers, Detectors and Associated Equipment*, vol. 555, no. 1-2, pp. 356–369, Dec. 2005. doi: [10.1016/j.nima.2005.08.106](https://doi.org/10.1016/j.nima.2005.08.106).
- [9] S. Dambach, U. Langenegger, and A. Starodumov, “Neutrino reconstruction with topological information”, *Nuclear Instruments and Methods in Physics Research Section A: Accelerators, Spectrometers, Detectors and Associated Equipment*, vol. 569, no. 3, pp. 824–828, Dec. 2006. doi: [10.1016/j.nima.2006.08.144](https://doi.org/10.1016/j.nima.2006.08.144).
- [10] G. Ciezarek, A. Lupato, M. Rotondo, and M. Vesterinen, “Reconstruction of semileptonically decaying beauty hadrons produced in high energy pp collisions”, *JHEP*, vol. 02, p. 021, 2017. doi: [10.1007/JHEP02\(2017\)021](https://doi.org/10.1007/JHEP02(2017)021).
- [11] “Determination of the quark coupling strength $|V_{ub}|$ using baryonic decays”, *Nature Physics*, vol. 11, no. 9, pp. 743–747, Jul. 2015. doi: [10.1038/nphys3415](https://doi.org/10.1038/nphys3415).
- [12] G. D’Agostini, “A multidimensional unfolding method based on bayes’ theorem”, *Nuclear Instruments and Methods in Physics Research Section A: Accelerators, Spectrometers, Detectors and Associated Equipment*, vol. 362, no. 2, pp. 487–498, 1995, ISSN: 0168-9002. doi: [https://doi.org/10.1016/0168-9002\(95\)00274-X](https://doi.org/10.1016/0168-9002(95)00274-X).

- [13] J. Harrison and C. T. H. Davies, “ $B \rightarrow D^*$ and $B_s \rightarrow D_s^*$ vector, axial-vector and tensor form factors for the full q^2 range from lattice QCD”, *Phys. Rev. D*, vol. 109, no. 9, p. 094 515, 2024. DOI: [10.1103/PhysRevD.109.094515](https://doi.org/10.1103/PhysRevD.109.094515).
- [14] G. Martinelli, S. Simula, and L. Vittorio, “What we can learn from the angular differential rates from semileptonic $B \rightarrow D^* \ell \nu \ell$ decays”, *Phys. Rev. D*, vol. 111, no. 1, p. 013 005, 2025. DOI: [10.1103/PhysRevD.111.013005](https://doi.org/10.1103/PhysRevD.111.013005).